Electronic Materials Letters, Vol. 9, No. 2 (2013), pp. 245-249
DOI: 10.1007/s13391-012-2175-y

Electrical Characteristics and Carrier Transport Mechanism for Ti/*p*-GaN Schottky Diodes

Seon-Ho Jang and Ja-Soon Jang*

Department of Electronic Engineering, LED-IT Fusion Technology Research Center (LIFTRC), Yeungnam University, Gyeongbuk 712-749, Korea

(received date: 27 September 2012 / accepted date: 3 December 2012 / published date: March 2013)

The temperature dependence of the electrical characteristics of non-alloyed Ti/*p*-GaN Schottky diodes was examined using current-voltage-temperature, turn-on voltage-temperature, and series resistance-temperature measurements. The thermal coefficient (K_j) and characteristic temperature (T_0) at $T \geq 293$ K were determined to be −4.1 mV/K and 65.06 K, respectively. The effective Schottky barrier height (SBH) was also determined to be 2.1 (±0.03) eV, which was in good agreement with the theoretical value. The possible carrier transport mechanisms at the interface are described in terms of the thermally decreased energy-band gap of *p*-GaN layers, thermally increased deep-level acceptor and increased further-activated-shallow-level acceptor. These were confirmed by the thermally increased ideality factor and high tunnelling parameter.

Keywords: Schottky diode, thermal coefficient, characteristic temperature, Schottky barrier height, carrier transport mechanism

1. INTRODUCTION

GaN-based semiconductors have attracted considerable attention for applications to light-emitting diodes (LEDs), ultraviolet Schottky barrier photodetectors, solar-blind Schottky photodiodes, metal-semiconductor field effect transistors and high electron mobility transistors on account of their superior material properties, such as wide band-gap, high breakdown field and high electron saturated velocity.[1-7] The formation of high-quality Schottky contacts is of technological importance for improving these devices. On the other hand, Mg-doped GaN layers grown on a sapphire substrate contain a high density of deep-level defects, originating from the low activation efficiency of Mg-H complexes.[8] In particular, a high defect density deteriorates the current-voltage (*I-V*) characteristics of *p*-GaN Schottky diodes (*p*-SDs) because the main current flow is affected considerably by these leakage components at the interface between the metals and *p*-GaN.[9-11] Until now, a variety of metallization schemes to realize high-quality *p*-SDs have been reported.[11-18] Nevertheless, few studies have examined high-quality *p*-SDs showing normal *I-V* characteristics. Recently, Jang *et al.*,[19] investigated high output power GaN-based LEDs with electrically-reverse connected *p*-SDs, and reported that the *p*-SD integrated LEDs are quite effective in reducing the forward leakage current if the *p*-SD has a normal *I-V* relationship. In their study, Cr/Al metallization schemes were assessed to form a *p*-SD, and Schottky behaviour were observed when the samples were annealed at 500°C for 30 sec in a flowing nitrogen ambience. In that case, however, the as-deposited contact showed leaky ohmic behaviour, suggesting that the formation of non-alloyed Schottky contacts on *p*-GaN is quite difficult due to the existence of a high density of deep-level defects in *p*-GaN.[8,19,26,27]

One of the SD technologies is how to interpret the Schottky barrier characteristics at the interface between the metal thin film and semiconductor. For Schottky contacts on *p*-GaN, the Schottky barrier characteristics were assumed to be governed by thermionic emission (TE) theory based on the *I-V* data.[9,10,12-17] In particular, the reported SBHs for Ni-based *p*-Schottky contacts showed a large discrepancy between the experimental and theoretical values ranging from 0.49 to 2.9 eV.[9,12,14-17] Yu *et al.*[20] suggested that the TE model is unsuitable for analyzing the barrier height because of the temperature independence of the tunnelling components of the *I-V* characteristics in metal/*n*-GaN Schottky contacts. In addition, Lin *et al.*[11] examined the application of a thermionic field emission (TFE) model to assess the SBH at the interface between Ni and *p*-GaN, and proposed that the TFE is valid for obtaining the SBH due to the large ideality factor ($n \gg 1$) originating from the high defect density in *p*-GaN.[8,10,11,19,26,27] Furthermore, for Schottky contacts on *n*-InGaN layers with a higher defect density,[21] the SBHs obtained from the TFE calculation were in good agreement with the theoretical values. Because the *p*-GaN layers contain

*Corresponding author: jsjang@ynu.ac.kr

relatively large amounts of deep-level acceptors, the use of the TFE model including a tunnelling parameter (E_{00}) is reasonable for obtaining the SBHs from the *p*-Schottky contacts. Although the TFE model based on the *I-V* characteristics is suitable for determining the SBH for Schottky contacts on *p*-GaN, further studies on the temperature dependence of the leakage current, series resistance, ideality factor and energy-band gap will be needed to improve the understanding of the current flow mechanism at the interface between the Schottky metal and *p*-GaN. This study examined the temperature dependence of the electrical properties of Ti/*p*-GaN SD using the turn-on voltage-temperature (V_{th}-T), series resistance-temperature (R_s-T) and leakage current-temperature (I_0-T) characteristics. The feasible carrier transport mechanisms are also discussed.

2. EXPERIMENTAL PROCEDURE

A metalorganic chemical vapour deposition system was used to grow a 2-μm-thick unintentionally-doped GaN layer on a 40-nm-thick GaN nucleation layer/(0001) sapphire substrate. This was followed by the growth of a 100 nm-thick Mg-doped GaN layer with a Mg concentration of 3×10^{19} cm^{-3}. The effective hole density of *p*-GaN was determined to be 3.4×10^{17} cm^{-3} using Hall measurements. Prior to the fabrication of the Schottky patterns, the surface of the GaN was degreased ultrasonically using acetone, methanol and ethanol for 5 min per step, and then rinsed with deionised water. Figure 1 shows a schematic cross-sectional diagram of the Schottky diode including Schottky and Ohmic patterns. The circular inner pattern means Schottky contact, and the outer pattern indicates ohmic contact. This was followed by a buffered oxide etching (BOE) surface treatment to remove the native oxide, which is quite harmful to high-performance GaN-based devices. Schottky contacts were fabricated on the surface-treated GaN using a photolithographic technique. For ohmic contact, Ni/Au (50/100 nm) layers were deposited by electron-beam evaporation and annealed at 500°C for 1 min in a flowing N_2 ambience. To form Schottky contacts, a Ti (50 nm) layer was deposited by e-beam evaporation under an ultrahigh vacuum of 2×10^{-7} Torr. The current-voltage (*I-V*) and current-voltage-temperature (*I-V-T*) data were obtained using a semiconductor analyzer (HP 4155A) and a probe station with a hot chuck system.

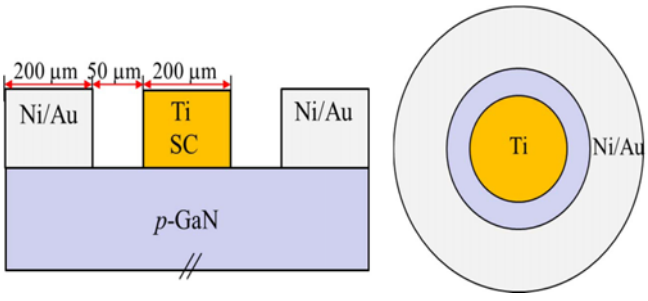

Fig. 1. Cross-sectional and top-view schematic diagrams of a Ti/*p*-GaN Schottky diode.

3. RESULTS AND DISCUSSION

Figure 2(a) shows the temperature dependence of the current-voltage (*I-V*) characteristics of Ti/*p*-GaN Schottky diode (SD). The rectifying *I-V* curve at room temperature was obtained, indicating the formation of non-alloyed Schottky contacts on *p*-GaN. Figure 2(a) also presents a possible equivalent circuit. The formation of non-alloyed SD could be due to the combined effects of the effective removal of native oxide and the deposition conditions. In preliminary work, the deposition rate and basal working pressure dependence of the device quality of Schottky diodes (data not shown) showed that electrical properties of *p*-Ti SD (on surface-treated GaN) are critically affected at a deposition rate ≤ 0.3 Å/sec and a basal working pressure ≤ 3×10^{-7} Torr,

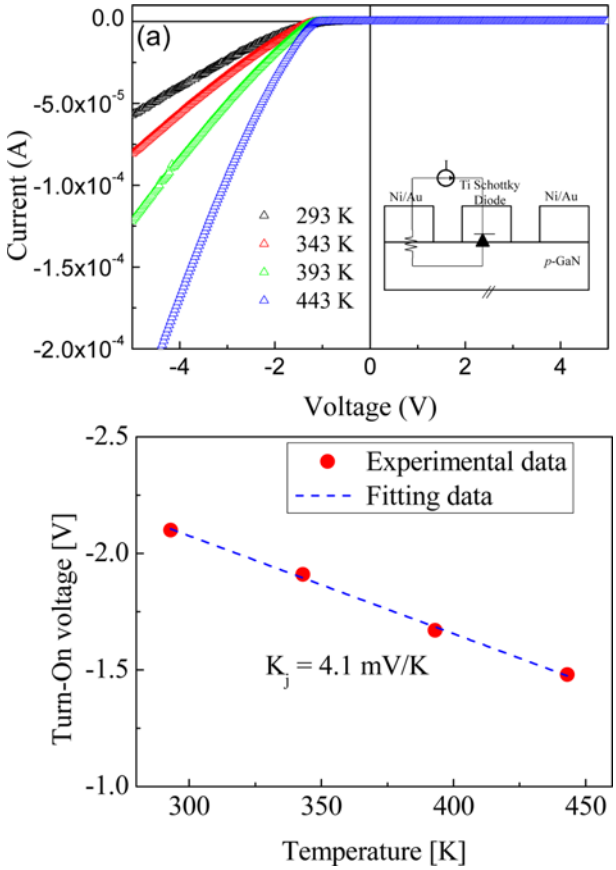

Fig. 2. (a) Temperature-dependent *I-V* characteristics of a Ti/*p*-GaN Schottky diode. The inset is the electrically equivalent circuit of the Schottky diode. (b) Plots of the temperature-dependence characteristics between the turn-on voltages and temperature. The close circles denote the experimental data. The dash lines indicate the theoretical data using equation (1). The thermal decay coefficient (K_j) was determined to be –4.1 mV/K.

even though both conditions are somewhat changeable for different metals, such as Cr and Ni. In addition, the effective removal of the native oxide on the *p*-GaN surface is also very important for obtaining high-performance SDs because the native oxide layer is a dominating factor that can give rise to an unwanted interface leakage current at the metal-semiconductor interface. Previous x-ray photoelectron spectroscopy (XPS) analysis (data not shown) showed that the BOE surface-treatment is quite effective in removing the native oxide of *p*-GaN, which is consistent with another report.[28]

Figure 2(b) shows the temperature dependence of the turn-on voltages ($V_{turn\text{-}on}$), which were obtained at a current of −10 μA. The $V_{turn\text{-}on}$ was reduced considerably from −2.08 V (at 293 K) to −1.53 V (at 443 K).

Thermal decay coefficient (K_j) for *p*-Schottky diode was obtained from a numerical fit using both the $V_{turn\text{-}on} - T$ data [as shown in Fig. 2(b)] and the following equation:[22]

$$K_j = -\frac{\Delta V_{turn\text{-}on}}{\Delta T}$$

$$= -\left(\frac{q(V_f - E_g)}{qT} + \frac{1}{q}\frac{dE_g}{dT} - \frac{3k}{q}\right) \quad (1)$$

where k is the Boltzmann constant, V_f is the turn-on voltage and E_g is the energy band-gap. This equation provides the basic temperature dependence of the $V_{turn\text{-}on}$. The first, second and third parts on the right-hand side of the equation are due to the temperature dependence of the carrier concentration, energy band-gap and effective density of states (DOS), respectively. Considering that the effective DOS has a relatively small temperature-dependence, Eq. (1) means that the thermally reduced $V_{turn\text{-}on}$ is subject to a reduced energy band-gap and an increased carrier concentration of the semiconductor. From the numerical fitting result shown in Fig. 2(b), K_j was determined to be −4.1 mV/K, which is relatively consistent with −2.3 mV/K for GaN-based LEDs.[22]

In Fig. 2(a), the *I-V* slopes, meaning the device series resistance (R_s), became stiffer with increasing T up to 443 K, indicating a decrease in the series resistance. The R_s and ideality factor (n) can be calculated using the following equation:[19]

$$\left|I\left(\frac{dV}{dI}\right)\right| = \left|IR_s + \frac{nkT}{q}\right| \quad (2)$$

where q is the charge and k is the Boltzmann constant. Figure 3 shows the calculation results. The R_s decreased exponentially and the corresponding n increased considerably with increasing T. Based on the exponential decay relationship between R_s and T, the relationship, [R_s α exp ($-T/T_0$)], was assumed, and the characteristic temperature (T_0) was found to be 65.06 K. The inverse proportion behaviour between R_s and n (as a function of T) reflects the increased carrier concentration in *p*-GaN directly.

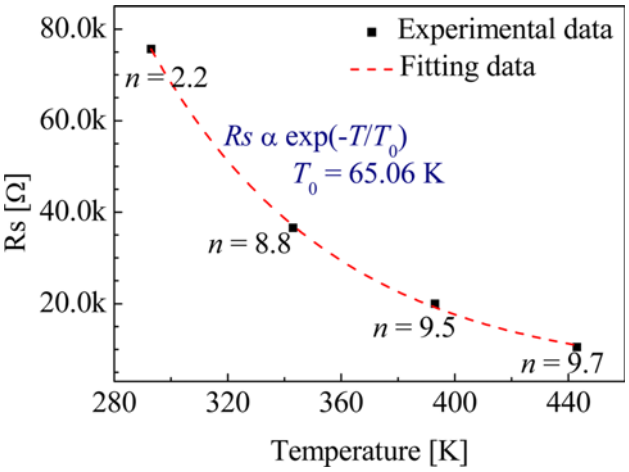

Fig. 3. Plots of the temperature-dependent R_s and n for a Ti/*p*-GaN Schottky diode. With increasing T, an inverse relationship between them was found. The dash lines mean the theoretical values obtained from the numerical fitting using the equation, [R_s α exp ($-T/T_0$)].

Leakage current-temperature (I_o-T) measurements were carried out to examine the current flow mechanism at the interface between Ti and *p*-GaN. The absolute leakage currents (I_0) were obtained under a bias of −0.05 V. In this study, the value of A^{**} was calculated theoretically to be 103.8α Acm^{-2}k^{-2} where the empirical factor (α) was obtained to be 0.12.[23] The SBHs ($q\Phi_B$) were not sensitively dependent on A^{**}.[11,18,23,24] The thermionic field emission (TFE) model was used to obtain the SBH and analyze the current transport at the interface using the I_0-T data. The TFE equations can be expressed as follows:[11,18,21,24]

For TFE conduction mode,

$$I = AJ_0 \exp\left[\frac{qV}{E_{00}\coth(E_{00}/kT)}\right] \quad (3)$$

$$J_0 = \frac{A^{**}T\sqrt{\pi E_{00}q(\phi_B - V - \xi)}}{k\cosh(E_{00}/kT)} \times$$

$$\exp\left[-\frac{q\xi}{kT} - \frac{q}{E_{00}\coth(E_{00}/kT)}(\phi_B - \xi)\right] \quad (4)$$

$$E_{00} = \frac{qh}{4\pi}\sqrt{\frac{N_a}{\varepsilon_s m^*}} \quad (5)$$

where A is the effective area of the Schottky diode (3.1×10^{-4} cm^2), E_{00} is the tunnelling parameter, A^{**} is the Richardson constant ($A^{**} = 120 \cdot \alpha \cdot (m^*/m_e)$), α is the empirical factor, h is the Planck constant, m^* is the effective mass of a semiconductor ($0.8m_e$),[8,11,23] ε_s is the dielectric constant of a semiconductor ($9.5\varepsilon_o$)[8,11,23] and ξ is the energy difference, $E_F - E_V$. Figure 4 shows plots of the experimental and theoretical

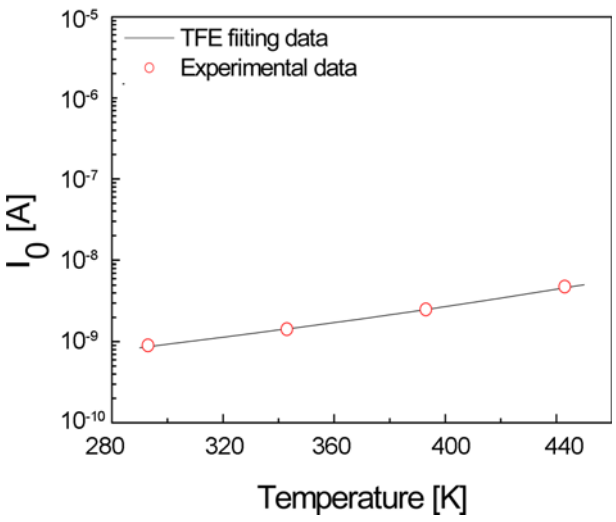

Fig. 4. Experimental and theoretical values of the leakage current (I_0) as a function of temperature based on the TFE equations. The lines denote the theoretical values.

values of I_0 as a function of T. The experimental results are in good agreement with the TFE fitting result, indicating that TFE conduction at ≥293 K is dominant for carrier flow at the interface. This result is consistent with those reported by Lin *et al.*[11] Numerical fitting revealed an effective SBH and E_{00} of 2.1 (±0.03) eV and 70 (±0.4) meV, respectively. The effective SBH (obtained from Fig. 4) was similar to the absolute value of $qV_{\text{turn-on}}$ (–2.08) eV measured at 293 K. In general, the SBH at the interface between a metal and *p*-semiconductor is determined using the energy difference of $[E_g - q(\Phi_m - \chi)]$ where $q\Phi_m$ is the metal work function and $q\chi$ is the electron affinity. When the parameters, such as $E_{g\_GaN} = 3.4$ eV,[8] $q\Phi_{Ti} = 4.3$ eV[25] and $q\chi = 3.3$ eV[8] at room temperature, were considered, $q\Phi_B$ was determined to be 2.4 eV. As the combined factors of the Schottky barrier lowering effect of 0.1 ~ 0.2 eV and the additional SBH reduction (by the effective removal of the native oxide[28]) were taken into account, the SBH (2.1 eV) obtained through the TFE fitting was consistent with that from the Schottky contact model. In addition, based on the E_{00}, the effective carrier concentration (N_{a_eff}) of *p*-GaN was calculated to be 7.4×10^{19} cm^{-3}, which is much larger than the Mg doping concentration (N_{Mg}) of 3×10^{19} cm^{-3}. The discrepancy between N_{a_eff} and N_{Mg} can be attributed to the existence of high accumulated deep-level defects near the *p*-GaN surface.[10,11]

Based on the results from Figs. 2-4, the thermally reduced turn-on voltage and series resistance can be explained as follows. First, the energy band-gap is reduced thermally and the shallow-level acceptors near the *p*-GaN surface are also activated further, as illustrated from Eq. (1) and Fig. 5. Second, a range of deep-level defects (near the *p*-GaN surface) induced by non-activated Mg-H complexes,[8] Ga vacancies and various point-defect complexes with a broad yellow energy band[26,27] and surface states[8,25-27] can occupy energy positions ranging from 0.2 eV to even 1.0 eV above the valence band of *p*-GaN. This means that the deep-level defects can act as a deep-level carrier. With increasing T, deep-level carriers go toward the Ti layer by carrier hopping, as illustrated in Fig. 5. The overall increased shallow- and deep-level carriers (confirmed by the thermally increased ideality factor and high tunnelling parameter) can cause a decrease in energy band-bending. Eventually, the combined effects of the thermal shrinkage of the energy band-gap and the increased shallow- and deep-level carriers can give rise to a decrease in the turn-on voltage and series resistance with increasing T. Accordingly, for *p*-SD at ≥293 K, some carriers experience tunnelling through the Schottky barrier and some carriers also flow across the barrier (Fig. 5).

4. CONCLUSIONS

In conclusion, this study examined the carrier flow mechanism of Ti/*p*-GaN ($N_a \sim 3.4 \times 10^{17}$ cm^{-3}) Schottky diodes

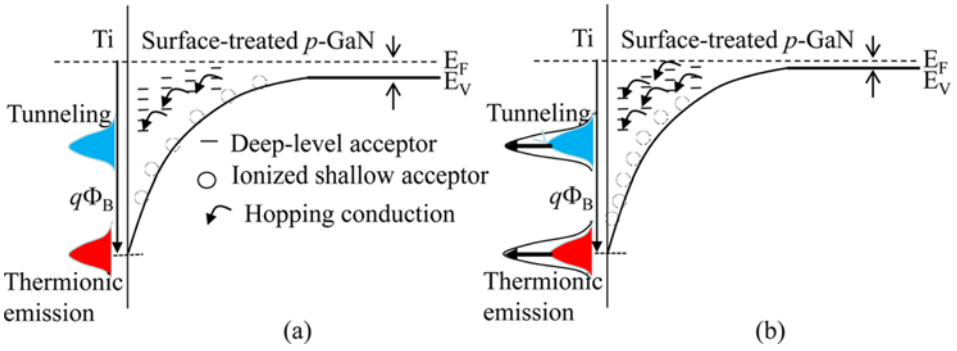

Fig. 5. Possible energy band diagram of the Ti/*p*-GaN interface; (a) 293 K and (b) 443 K. The comparisons indicate that the deep-level-assisted tunnelling (through hopping conduction) is enhanced and the thermally activated shallow carriers (or acceptors) are increased with increasing T. In addition, the energy difference in ($E_F - E_V$) is also reduced. Therefore, the tunnelling and thermionic emission are dominant for the carrier flow at the interface.

by examining the relationships between the thermal decay coefficient, series resistance-temperature and leakage current-temperature. The thermal coefficient (K_j) and characteristic temperature (T_0) were determined to be –4.1 mV/K and 65.06 K at $T \geq 293$ K, respectively. The effective Schottky barrier height ($q\Phi_B$) was also determined to be 2.1 (±0.03) eV, which is in good agreement with the theoretical value. For the Ti/*p*-GaN SD at $T \geq 293$ K, the carrier transport was governed by TFE conduction because of the combined effects of thermal shrinkage of the *p*-GaN band-gap and the increase in the shallow- and deep-level carriers, which were confirmed by the thermally increased ideality factor and high tunnelling parameter. These findings are expected to be useful for developing high-performance *p*-Schottky diodes and related optoelectronic devices.

ACKNOWLEDGEMENTS

This study was supported in part by the MKE through the industrial infrastructure program under Grant No. 10033630 and through the part and material development program under Grant No. 211C000553. This research was also partially supported by the MEST and NRF through the Human Resource Training Project for Regional Innovation.

REFERENCES

1. M. A. Khan, A. Bhattarai, J. N. Kuznia, and D. T. Olson, *Appl. Phys. Lett*. **63**, 1214 (1996).
2. S. Nakamura, M. Senoh, N. Iwasa, and S. Nagahama, *Jpn. J. Appl. Phys. Part 2* **34**, L797 (1995).
3. M. A. Khan, J. N. Kuznia, A. R. Bhattarai, and D. T. Olson, *Appl. Phys. Lett*. **62**, 1786 (1993).
4. N. Biyikli, O. Aytur, I. Kimukin, T. Tut, and E. Ozbay, *Appl. Phys. Lett*. **81**, 3272 (2002).
5. Z. Vashaei, E. Clicek, C. Bayram, R. McClintock, and M. Razeghi, *Appl. Phys. Lett*. **96**, 201908 (2010).
6. S.-Y. Jung and T.-Y. Seong, *Electron. Mater. Lett.* **8**, 549 (2012).
7. A. Mao, J. Cho, E. Fred Schubert, J. K. Son, C. Sone, W. J. Ha, S. Hwang, and J. K. Kim, *Electron. Mater. Lett*. **8**, 1 (2012).
8. J. Wu, *J. Appl. Phys.* **106**, 011101 (2009).
9. K. Shiojima, T. Sugahara, and S. Sakai, *Appl. Phys. Lett*. **77**, 4353 (2000).
10. J. S. Kwak, O. H. Nam, and Y. Park, *J. Appl. Phys.* **95**, 5917 (2004).
11. Y. J. Lin, *Appl. Phys. Lett*. **86**, 122109 (2005).
12. L. S. Yu, D. Qiao, L. Jia, S. S. Lau, Y. Qi, and K. M. Lau, *Appl. Phys. Lett*. **79**, 4536 (2001).
13. X. A. Cao, S. J. Pearton, G. Dang, P. A. Zhang, F. Ren, and J. M. VanHove, *Appl. Phys. Lett*. **75**, 4130 (1999).
14. P. J. Hartlieb, A. Roskowski, R. F. Davis, W. Platow, and R. J. Nemanich, *J. Appl. Phys*. **91**, 732 (2002).
15. K. Shiojima, T. Sugahra, and S. Sakai, *Appl. Phys. Lett*. **74**, 1936 (1999).
16. K.-P. Hsueh, H.-T. Hsu, C.-M. Wang, S.-C. Huang, Y.-M. Hsin, and J.-K. Sheu, *Appl. Phys. Lett*. **87**, 232107 (2005).
17. T. Mori, T. Kozawa, T. Ohwaki, Y. Taga, S. Naagai, S. Yamasaki, S. Asami, N. Shibata, and M. Koike, *Appl. Phys. Lett.* **69**, 3537 (1996).
18. L. Stafford, L. Voss, S. J. Pearton, J.-J. Chen, and F. Ren, *Appl. Phys. Lett.* **89**, 132110 (2006).
19. J.-S. Jang, *Appl. Phys. Lett*. **93**, 081118 (2008).
20. L. S. Yu, Q. Z. Liu, Q. J. Xing, D. J. Qiao, S. S. Lau, and J. Redwing, *J. Appl. Phys*. **84**, 2099 (1998).
21. J.-S. Jang, D. Kim, and T.-Y. Seong, *J. Appl. Phys.* **99**, 073704 (2006).
22. Y. Xi and E. F. Schubert, *Appl. Phys. Lett*. **85**, 2163 (2004).
23. J.-S. Jang and T.-Y. Seong, *Appl. Phys. Lett*. **76**, 2743 (2000).
24. T. Nam, J.-S. Jang, and T.-Y. Seong, *Current Appl. Phys*. **12**, 1081 (2012).
25. S.-H. Jang and J.-S. Jang, *Electrochem. Solid-State Lett*. **13**, H403 (2010).
26. J. Neugebauer and C. G. Van de Walle, *Appl. Phys. Lett*. **64**, 503 (1996).
27. T. Mattila and R. M. Nieminen, *Phys. Rev. B* **55**, 9571 (1997).
28. J.-S. Jang and T.-Y. Seong, *J. Appl. Phys*. **88**, 3064 (2000).